

## Paper 102- Performance of Advanced Materials and Details during the Shake Table Tests of a 4-Span Bridge Model

Carlos A. Cruz-Noguez<sup>1</sup> and M. “Saiid” Saiidi<sup>2</sup>

<sup>1</sup> Research Associate, Dept. of Civil and Environmental Engineering, Univ. of Nevada, Reno, Reno, USA

<sup>2</sup> Professor, Dept. of Civil and Environmental Engineering, Univ. of Nevada, Reno, Reno, USA

**ABSTRACT:** As part of a major study on the seismic response of bridge systems with conventional and advanced details, a large-scale model of a four-span bridge incorporating several innovative plastic hinges was recently tested on the shake tables at the University of Nevada, Reno. The bridge model was subjected to a series of two-horizontal components of simulated earthquake records of the 1994 Northridge earthquake in California. The experimental results obtained during the seismic tests showed that, besides being effective in reducing permanent displacement of the bridge and damage at the plastic hinges, the high-performance materials and details substantially reduced the damage and modified significantly other response parameters of the bents compared to conventional reinforced-concrete (RC) construction. Increased ductility was observed in the pier with SMA/ECC combination and larger load capacity was exhibited by the pier with elastomeric pads. While rotations at the plastic hinges detailed with high-performance materials were significantly larger than those measured at plastic hinges made of conventional RC, the measured residual strains in the longitudinal reinforcement in the plastic hinges detailed with innovative details were smaller than those observed in RC plastic hinges. In terms of dynamic properties, the fundamental periods of the piers detailed with elastomeric bearings and super elastic memory alloys were slightly larger than the pier with post-tensioned columns.

### 1 INTRODUCTION

In non-critical bridges, prevention of collapse is the main performance objective under strong earthquakes. A new approach to earthquake-resistant concrete bridge design is emerging in which the “no-collapse” target performance is considered to be inadequate, and non-critical bridges are to remain functional or nearly so after strong earthquakes. For bridges to continue to be functional the column damage (damage indicator 1) should be none or minimal and permanent lateral displacements (damage indicator 2) should be very small. The use of high-performance materials and innovative details to address these indicators was recently investigated in the seismic test of a 33-m, quarter-scale bridge model conducted at shake table

laboratory of the University of Nevada, Reno (Cruz and Saiidi, 2010). The bridge model included six columns, each pair of which utilized a different unconventional detail at bottom plastic hinges: super elastic shape memory alloys (SMA) combined with engineered cementitious composites (ECC), post-tensioned columns, and columns with built-in elastomeric bearings. The upper plastic hinges were of conventional reinforced concrete (RC) construction to provide a direct comparison between the two types of construction. A 3-D rendering of bridge model is shown in Figure 1. The total length of the deck was 32.62 m, while the length of the outer spans was 7.47 m and that of the inner spans was 8.84 m. The deck was 2.29 m wide and 0.36 m thick. The clear column heights in all three bents were 1.83 m. Test results showed that the residual displacements in all three piers were insignificant and that the plastic hinges detailed with innovative materials showed no damage. This paper focuses on the performance of the advanced materials and details during the shake-table tests. The results are discussed in terms of the force-displacement response of the piers, strains exhibited by the longitudinal reinforcement at plastic hinges, rotational deformations of the columns, and the variation of the dynamic properties of the bridge during the seismic tests.

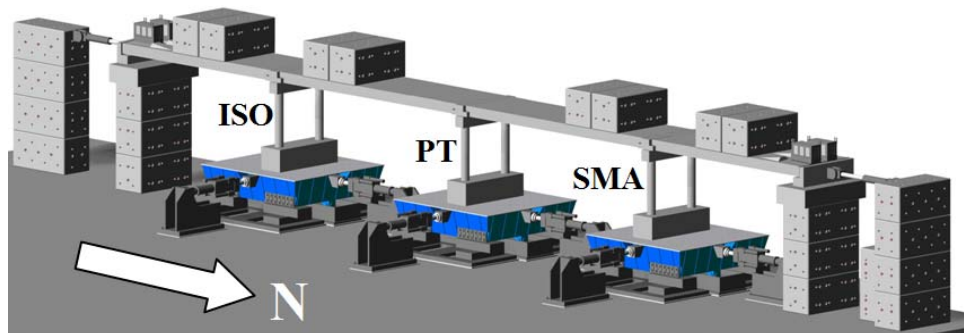


Figure 1. Test setup for the 4-span innovative bridge model.

## 2 COLUMN DESIGN

Three types of unique materials and details were used each in one of three piers of the bridge (Figure 2). In the pier labeled as SMA bent, the plastic hinges at the bottom of the columns were detailed with superelastic shape memory alloys and polyvinyl fibers mixed with a cement mortar, ECC. The SMA material was selected because of its ability to undergo large strains but recover its shape upon stress removal (Wilson and Wesolowsky, 2005) while ECC was chosen due to its enhanced ductility and high tensile strain capacity, as discussed by Li et al. (2000) and Fischer and Li (2003). In the middle pier, labeled PT bent, the columns were post-tensioned to provide recentering capability for the columns. Post-tensioning has been demonstrated to reduce permanent drifts in columns subjected to earthquake loading (Sakai and Mahin, 2004). In the bent with elastomeric pads, labeled as ISO bent, a built-in rubber pad was used to replace concrete in the bottom plastic hinges of columns to avoid concrete damage. The design of the rubber pad was a variant of that discussed by Kawashima and Nagai (2002) and modified by incorporating steel shims to prevent bar buckling and a central steel pipe to transmit shear.

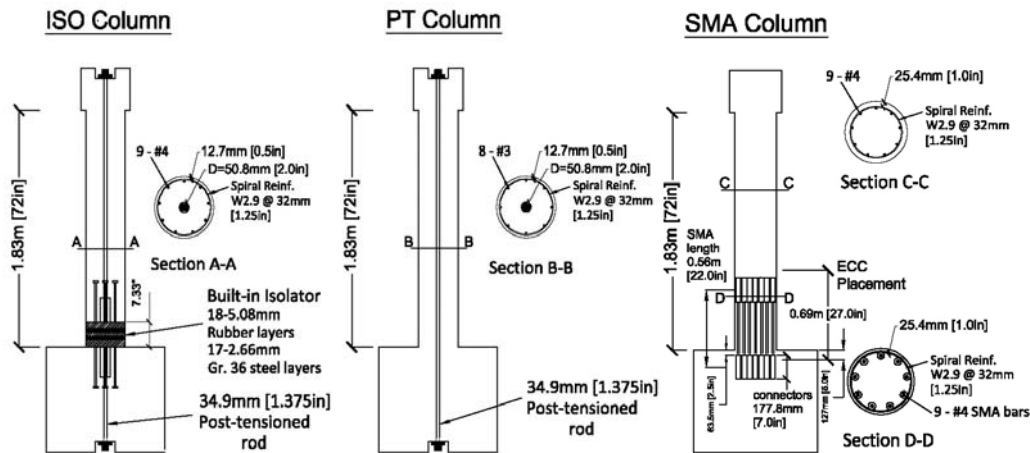


Figure 2. Side-view column basic details.

### 3 LOADING PROTOCOL

Seven coherent, runs of increasing amplitudes of the Northridge earthquake (1994) with peak ground acceleration (PGA) varying from 0.075 to 1.00g in the transverse direction and 0.10 to 1.00g in the longitudinal direction were applied to the model. Table 1 lists the amplitude of the motions used in pretests analytical studies and the target amplitude of the motions that were actually simulated in the shake tables. Note that only the transverse component of excitation was applied to the bridge during Runs 6 and 7 due to extensive damage observed at the top of the ISO and PT columns. In addition to the earthquake tests, white noise tests with a PGA of approximately 0.1g were conducted between earthquake tests to monitor the variation of the dynamic properties of the bridge in the transverse and longitudinal directions.

Table 1. Loading protocol

Component	Scaled PGA (g)						
	Run 1	Run 2	Run 3	Run 4	Run 5	Run 6	Run 7
Transverse	0.075	0.15	0.25	0.5	0.75	1.00	1.00
Longitudinal	0.1	0.2	0.33	0.66	1.00	0.00	0.00

### 4 PERFORMANCE OF ADVANCED MATERIALS AND DETAILS

#### 4.1 Force-displacement response of piers

Envelopes of the cumulative hysteretic force-displacement response for each bent are presented in Figure 3. Fracture of the longitudinal bars at the top plastic hinge of ISO bent columns and fracture of a spiral at the bottom plastic hinge in one of the PT columns during Run 7 were assumed to constitute failure of the bridge model. While the forces at the effective yield displacement were similar, the bent with the largest load capacity in both the transverse and longitudinal directions was the ISO bent, and the smallest load capacity was exhibited by the SMA bent. Comparable displacements were achieved at the three piers.

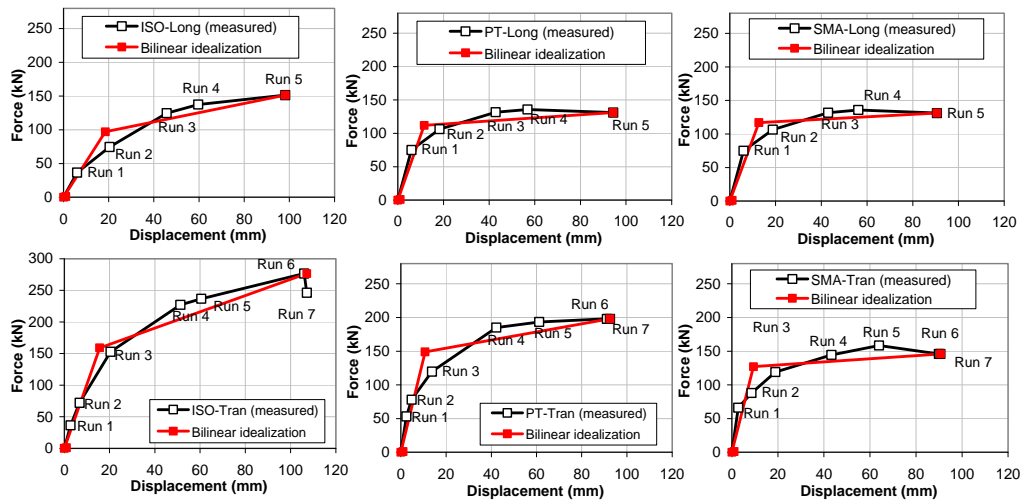


Figure 3. Force-displacement envelopes measured during Runs 1-7.

The maximum drifts of 5.86%, 5.06% and 4.96% in the transverse directions were recorded during Run 7 for the ISO, PT and SMA bents, respectively. In the longitudinal direction, the maximum drifts for the same bents measured during Run 5 were 5.37%, 5.16% and 4.96%, respectively. Bilinear idealizations of the envelopes of the hysteretic force-displacement response measured during the tests at the ISO, PT and SMA bents (Figure 3) led to displacement ductilities in the longitudinal direction of 5.3, 8.1 and 7.1, respectively. No failure of the bents was observed during Run 5 in the longitudinal direction. In the transverse direction the ductilities were 6.9, 8.6 and 9.6, respectively, in the ISO, PT, and SMA bents. As discussed by Cruz and Saiidi (2010), ISO and PT bents failed in the transverse direction during Run 7 while the SMA preserved its structural integrity. This indicates that the ductility capacity of the SMA bent was the largest and that of the ISO bent the smallest.

#### 4.2 Rotational deformations of plastic hinges

Column rotations were determined using the measured displacements on opposite sides of the plastic hinges. The rotations at the upper part of the columns were measured using gauge lengths of 152.4 mm. Since different gauge lengths were utilized to measure rotations at the bottom plastic hinges (Cruz and Saiidi, 2010), to compare among different plastic hinges the measured rotations were converted to rotations tributary to segments equal to 152.4 mm. Table 2 shows the maximum rotations at the different plastic hinges of the bridge. It is seen that rotations in SMA columns were the largest compared with conventional RC plastic hinges (top of ISO and SMA columns) and PT plastic hinges during Runs 1 to 5. At the bottom of the ISO columns, however, smaller rotations compared with the top were obtained because at the lower part of the column the rotations are distributed over a larger distance (the height of the pad). If the total rotation measured along the height of the pad (196.3 mm) was considered, the maximum rotation at the plastic hinge detailed with the elastomeric pad would exceed by 20% the maximum rotation measured at the top plastic hinge. On the other hand, the large rotations in the conventional plastic hinges at the top of the ISO and PT columns during 6 and 7 are attributed to considerable concrete damage and the reduced section. These rotations did not indicate the rotation capacity of the plastic hinges because the hinges had failed in Runs 6 and 7. Comparison of the apparent damage in innovative plastic hinges with that of conventional plastic hinges revealed that there was no damage in the elastomeric pads and the damage in the

SMA/ECC plastic hinges was minimal, whereas the damage in conventional reinforced concrete hinges was substantial despite the larger rotation of innovative hinges.

Table 2. Measured rotations at plastic hinges

Bent	SMA Bent				PT Bent				ISO Bent			
	Longitudinal		Transverse		Longitudinal		Transverse		Longitudinal		Transverse	
	Top	Bottom	Top	Bottom	Top	Bottom	Top	Bottom	Top	Bottom	Top	Bottom
1	0.0013	0.0013	0.001	0.0011	0.001	0.0014	0.0006	0.0006	0.0004	0.0026	0.0017	0.0011
2	0.0033	0.0059	0.0033	0.0052	0.0016	0.0043	0.0013	0.0016	0.0007	0.0059	0.0016	0.0025
3	0.0058	0.0193	0.0064	0.0123	0.0033	0.0115	0.0047	0.0063	0.0018	0.012	0.0052	0.0069
4	0.0074	0.0271	0.0098	0.0273	0.0061	0.0182	0.0179	0.0196	0.0024	0.0171	0.022	0.0198
5	0.0166	0.0472	0.0209	0.0362	0.0176	0.038	0.0264	0.0298	0.0058	0.0247	0.0287	0.022
6	---	---	0.0272	0.0431	0.0054	0.0121	0.0392	0.0429	0.0027	0.0035	0.0586	0.0369
7	---	---	0.0222	0.0478	0.0056	0.0134	0.0406	0.0457	0.0031	0.0031	0.0562	0.0378

--- Rotation was not measured due to malfunction of sensor

### 4.3 Longitudinal reinforcement strains

The transverse bent shear versus the longitudinal bar strain response during Runs 1-7 is shown in Figure 4 for both top and bottom plastic hinges in all the bents at the ISO, PT and SMA bents on the east or west faces of the columns (the areas of maximum strain for loading in the transverse direction of the bridge model). The bars with the largest strain measurements in each column were chosen for comparison. One of objectives of using advanced materials was to reduce residual strains in the reinforcement, which lead to residual lateral drift. It is seen that the residual strains in the SMA bars were considerably smaller than those measured in the steel bars, as expected (SMA residual strains were 25% of the steel residual strains during the rare earthquake, Run 5). It is also possible to notice the distinct energy dissipation capacity of the SMA bars compared with steel. The steel bars dissipated nearly 2 times more energy than SMA bars. In the PT bent, the residual strains at the bars were 31% of those recorded at the steel bars located in similarly reinforced sections in the SMA bent due to the recentering action provided by the PT rods. In the ISO bent, the residual strains at the bars in bottom plastic hinges (detailed with the elastomeric pad) were 32% of those recorded in the bars at the top plastic hinges (detailed with RC) due to the recentering action of the PT rods and the unbonding of the bars at the bottom plastic hinges.

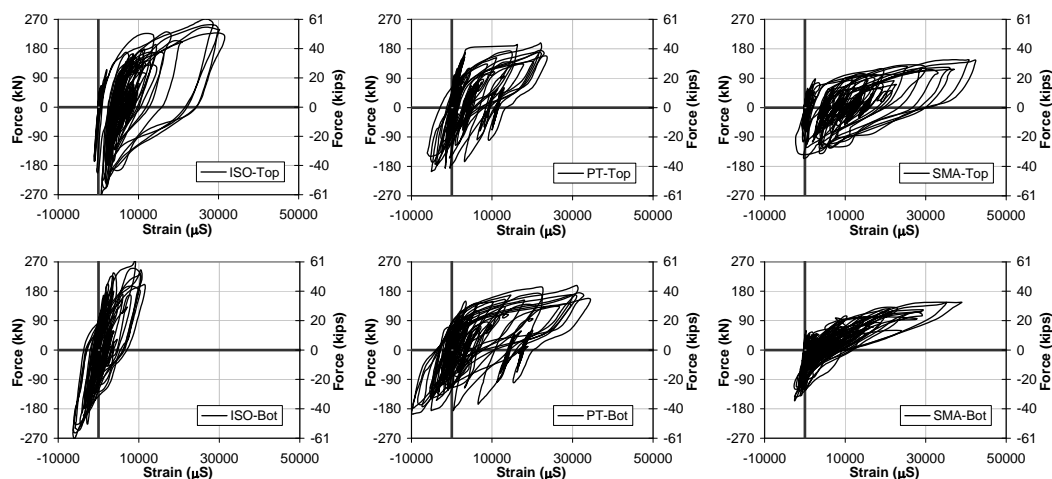


Figure 4. Hysteretic Bent Shear-Strain Relationships for longitudinal reinforcement.

#### 4.4 Post-tensioning tendons

Since the tendons were designed to remain elastic throughout the tests, it was important to investigate their actual axial force variations during the shake table simulations. According to the information provided by the supplier, the post-tensioning rods used in this study would yield at 978.6kN. Figure 5 presents plots of post-tensioning force versus resultant displacement at top of bents for the rods in the west columns of the ISO and PT bents. These columns experienced the largest variation of axial force and the maximum variation occurred during Runs 5 and 6. Note that the SMA bent was not post tensioned. The maximum recorded forces in the rod in the ISO column occurred during Run 6, with 513.5kN and in the PT column occurred during Run 5 with 768.8 kN. As intended, the measurements indicate that the rods remained elastic. It is seen that the variation of force in the tendons at the ISO column was less pronounced than that of the tendons at the PT column. This is because the elastomeric pads at the bottom of ISO columns allow for larger axial deformations, thus limiting the build-up of axial forces developed in the tendons in that bent.

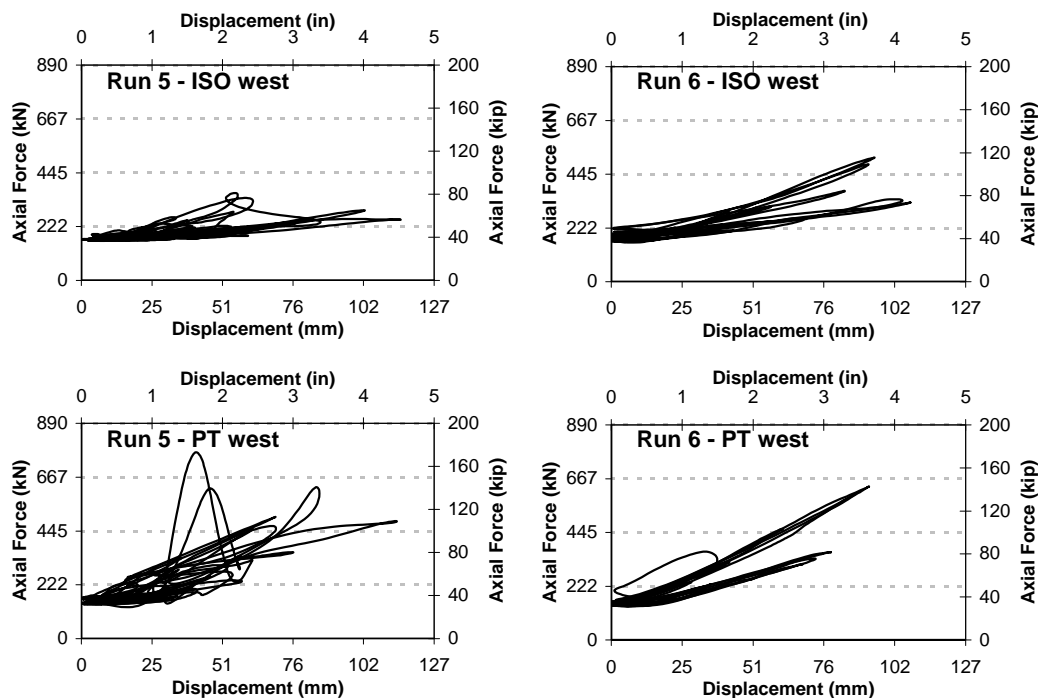


Figure 4. Axial force – resultant displacement plots for post-tensioned rods.

#### 4.5 Variation of dynamic properties of the bridge

To track damage progression during the experiments, the model was excited using white noise motion at the shake tables with frequency content from 0 – 30Hz and PGA of approximately 0.1g and the vibration periods were estimated. To eliminate the frequency contribution from the shake table movement and to identify only the frequencies being amplified by the bridge, the spectrum calculated for each bent was divided by the spectrum calculated for the shake table supporting that bent. The variation of the fundamental periods in the transverse direction for all

the bents is shown in Table 3. Results corresponding to the longitudinal direction are not given in Table 3 since the spectral analysis indicated no clear amplification of frequencies for that component of movement. Also it should be noted that the high rigidity of the superstructure coupled the movements of the bents, leading to comparable frequencies. It is seen that all bents exhibited the same initial period of 0.258 s (WN0) indicating comparable initial stiffness in the transverse direction. The fundamental period during the next four white noise tests (WN1 to WN4) in PT bent did not increase at the same rate as that of ISO and SMA bents. The presence of post-tensioning forces is believed to help reducing crack opening under low-amplitude motions, and hence the stiffness of the PT columns was relatively high leading to shorter periods. The post-tensioning forces in the ISO bent did not have the same effect because the reduced axial stiffness of the elastomeric pads prevented build up of large post-tension forces and overall cracking of the ISO bent was less extensive. Both ISO and SMA bents had nearly the same periods in all white noise tests. For the final white noise tests, WN7, all bents exhibited the same period (0.372 s). This is reasonable because all the bents had entered the plastic range and had softened substantially. As a result the superstructure moved as a rigid body in the transverse direction, imposing similar motions in all the bents.

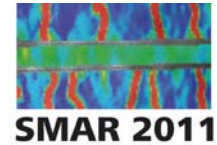
Table 3. Fundamental bent periods

Periods (s) in the transverse direction			
Test	Bent		
	ISO	PT	SMA
WN0 (prior to Run 1)	0.258	0.258	0.258
WN1 (after Run 1)	0.267	0.258	0.262
WN2 (after Run 2)	0.271	0.267	0.271
WN3 (after Run 3)	0.291	0.286	0.308
WN4 (after Run 4)	0.326	0.308	0.326
WN5 (after Run 5)	0.314-0.400	0.314-0.400	0.314-0.400
WN6 (after Run 6)	0.372	0.364	0.372
WN7 (after Run 7)	0.372	0.372	0.372

## 5 CONCLUSIONS

The following conclusions are the main findings of the experimental studies reported in this paper:

- a) The ductilities achieved by the bents with innovative details were comparable to those observed in RC piers designed to sustain strong nonlinear actions. This is an attractive feature when implementing these advanced materials in real bridge structures.
- b) The rotational deformations exhibited by the plastic hinges detailed with SMA/ECC were higher than those measured for the RC plastic hinges. For similar gauge lengths, the rotation at the plastic hinges with elastomeric pads was smaller than those detailed with RC. If the total rotation along the height of the pad were considered, the rotation at the bottom of the ISO columns would be larger than the upper part made with RC.
- c) The design objective of keeping the post-tensioned rods elastic in the PT and ISO bridge columns was achieved. The recentering action of the post-tensioned rods helped minimize the permanent deformations in the PT and ISO columns.
- d) The residual strains in the longitudinal reinforcement were effectively reduced by the innovative materials incorporated at the plastic hinges. This contributed to minimizing the residual displacements in the bridge.



## 6 REFERENCES

Cruz-Noguez, C. A. and Saiidi, M. Experimental and Analytical Seismic Studies of a Four-Span Bridge System with Innovative Materials. Technical Rep. No. CCEER-10-04, Center for Civil Engineering Earthquake Research, Dept. of Civil Engineering, Univ. of Nevada, Reno, Nev. September 2010.

Wilson, J.C., and Wesolowsky, M. Shape memory alloys for seismic response modification: a state-of-the-art review. *Earthquake Spectra*, 21(2), 2005, pp. 569-601.

Li, V., Horii, H., Kabele, P., Kanda, P., and Lim, Y. M. Repair and retrofit with engineered cementitious composites. *Engineering Fracture Mechanics*, No. 65, 2000, pp. 317-334.

Fischer, G., and Li, V.C. Deformation behavior of fiber-reinforced polymer reinforced engineered cementitious composite (ECC) flexural members under reversed cyclic loading conditions. *ACI Struct. J.*, 100(1), 2003, pp. 25-35.

Sakai, J. and Mahin, S. A. Analytical investigations of new methods for reducing residual displacements of reinforced concrete bridge columns. PEER-2004/02, Pacific Earthq. Engrg. Res. Center, Univ. of California at Berkeley, California, 2004.

Kawashima, K. and Nagai, M. Development of a reinforced concrete pier with a rubber layer in the plastic hinge region. *Proc. JSCE, Structural and Earthquake Engineering*, 703/I-59, 2002, pp. 113-128.